Scholars Journal of Engineering and Technology

OPEN ACCESS

Abbreviated Key Title: Sch J Eng Tech
ISSN 2347-9523 (Print) | ISSN 2321-435X (Online)
Journal homepage: https://saspublishers.com

A Theoretical Study of the Fragmentation Mechanism of Deprotonated Alanine (DFT)

Quan Sun[1*], Hongjie Qu[1], Qiang Li[1], Dongxue Ding[1], Lili Cao[1], Jingyu Pang[1], Bo Wang[1]

[1]College of Science, Heilongjiang Bayi Agricultural University, Daqing, 163319, Heilongjiang Province, P.R. China

DOI: 10.36347/sjet.2022.v10i07.007 | **Received:** 11.06.2022 | **Accepted:** 23.07.2022 | **Published:** 27.07.2022

***Corresponding author:** Quan Sun
College of Science, Heilongjiang Bayi Agricultural University, Daqing, 163319, Heilongjiang Province, P.R. China

Abstract | **Review Article**

In this paper, density functional theory (DFT) was applied to study the isomerization process and fragmentation mechanism of deprotonated alanine ions ([β-Ala–H]$^-$) at B3LYP/6-311++G (2df, 2pd) level. Deprotonated α-alanine ions generally have lower energies than deprotonated β-alanine ions, and **1a2** is the most stable structure. In the isomerization process, the reaction barrier ($\Delta G^{\neq}$) required for hydrogen transfer is the highest, that the pathway of NH_3- loss reaction to the product **p3** is the only forward spontaneous reaction in thermo dynamics and NH_3-loss reaction is also easier than H_2O-loss reaction in kinetics. Meanwhile, the effect of temperature on the optimal H_2O- and NH_3-loss reaction paths of the deprotonated α- and β-alanine ions were investigated, and the results showed that temperature had little effect on H_2O- and NH_3-loss reactions. In addition, different calculation methods and focus analysis of the basis group were investigated, and the results show that B3LYP/6-311++G (2df, 2pd) level is suitable for this study.

Keywords: deprotonated alanine ions, reaction mechanism, H_2O-loss reaction, NH_3-loss reaction.

1. INTRODUCTION

Alanine is one of the simplest non-essential amino acids [1], which can be divided into α- and β- because of the position of the amino group on the carbon chain. Among them, α- -alanine exists *D*- and *L*-racemate [2]. α- and β-alanine play an important role in the metabolism of plants and animals [3, 4], and β-alanine plays a role in the regulation of nerve [5] and vision [6]. So far, alanine has been of great significance in the fields of organic synthesis [7, 8], pharmaceutical chemistry [9, 10], medical detection [11], functional beverage [12, 13] and astrochemistry [14, 15].

At the end of the 20th century, the gas phase structures of α- and β-alanine were discovered by Godfrey [16, 17] and McGlone [18], respectively, and their corresponding solutions [19, 20] and crystal [21, 22] structures were in the form of zwitter ions. In 1989, Eckersley [23] *et al*, first used fast atomic bombardment mass spectrometry (FAB-MS/MS) to obtain dehydrated [Ala–H–H_2O]$^-$ and deaminated [Ala–H–NH_3]$^-$ fragments of deprotonated alanine ([Ala–H]$^-$). However, twenty years later, Choi [24] applied atmospheric pressure chemical ionization mass spectrometry (APCI-MS) and failed to dissociate the corresponding fragments, and the fragmentation mechanism is still unknown.

Based on a series of previous studies on the mechanism of the deprotonated amino acids [25], the geometric configurations of the reactants, intermediates, transition states, product ions and neutral molecules of [Ala–H]$^-$ were optimized, the thermodynamic data were obtained by frequency analysis. The potential energy profiles of isomerization, H_2O- and NH_3-loss pathways of [Ala–H]$^-$ were constructed respectively, and then judge the dominant pathway and the dominant product. In addition, the influence of temperature on H_2O- and NH_3-loss pathways of [Ala–H]$^-$ is analyzed, and the rationality of the research plan was explored from different levels of focal-point analyze (FPA) [26] in this study. The results will provide some model support for clarifying the fragmentation mechanism of deprotonated amino acid ions.

2. COMPUTATIONAL DETAILS

Imparity with β-alanine, β-alanineis not chiral. Therefore, [β-Ala–H]$^-$ is constructed directly as the investigated target in this study. The geometric configurations of all reactants, intermediates, transition

states, products and dissociated neutral molecules were obtained by using B3LYP method [27] combined with 6-31G base set [28] in corporated in the Gaussian09 program system [29]. After geometric optimization, frequency vibration calculation is carried out to determine the geometrical position is the minimum value (no virtual frequency) or transition state (only one virtual frequency). In addition, we also calculate the thermal correction of the key stability points at the same level in geometric optimization, and obtain their relative enthalpy of reaction and Gibbs free energy of relative reaction with temperature, and the FPA [26] of the rate-determine steps were calculated.

3. RESULT AND DISCUSSION

3.1 Isomerization of [Ala–H]⁻

A total of 51 isomers of the deprotonated α- and β-alanine have been calculated in this study. According to the position of negative charge, whether the molecule is cycloforming or not, and the *cis-trans* isomerism of the cyclo forming molecule, these 51 isomers can be divided into 8 species, among which **1a**, **1b, 1c** belong to [α-Ala–H]⁻, **2a, 2b, 2c** belong to [β-Ala–H]⁻, **d** and **e** are the "bridge anions" linking the deprotonated α- and β -alanine ions. All the relative Gibbs free energies (R.G., kcal·mol^{-1}) are based on **1a2**, the lowest energy of [Ala–H]⁻ isomers, as the reference point.

Figure 1 shows the isomerization process of the deprotonated α- and β-alanine. Among them, **1a** and **2a** negative ions have the lowest energies (R.G., 0.00 ~ 7.54 kcal·mol^{-1}), which negative charge position is on CO_2. The negative ions **1b** and **2b** have higher energies (R.G., 26.25 ~ 34.65 kcal·mol^{-1}), which their negative charge positions are on α-C. The energies of **1c, 2c, d** and **e** are the highest, and the energies of these three species of anions are similar to each other (R.G., 50.35 ~ 64.53 kcal·mol^{-1}), which negative charge of species **c** is on β-C, negative charge of species **d, e** on oxygen atom, and the two kinds of negative ions are *cis-trans* isomerism.

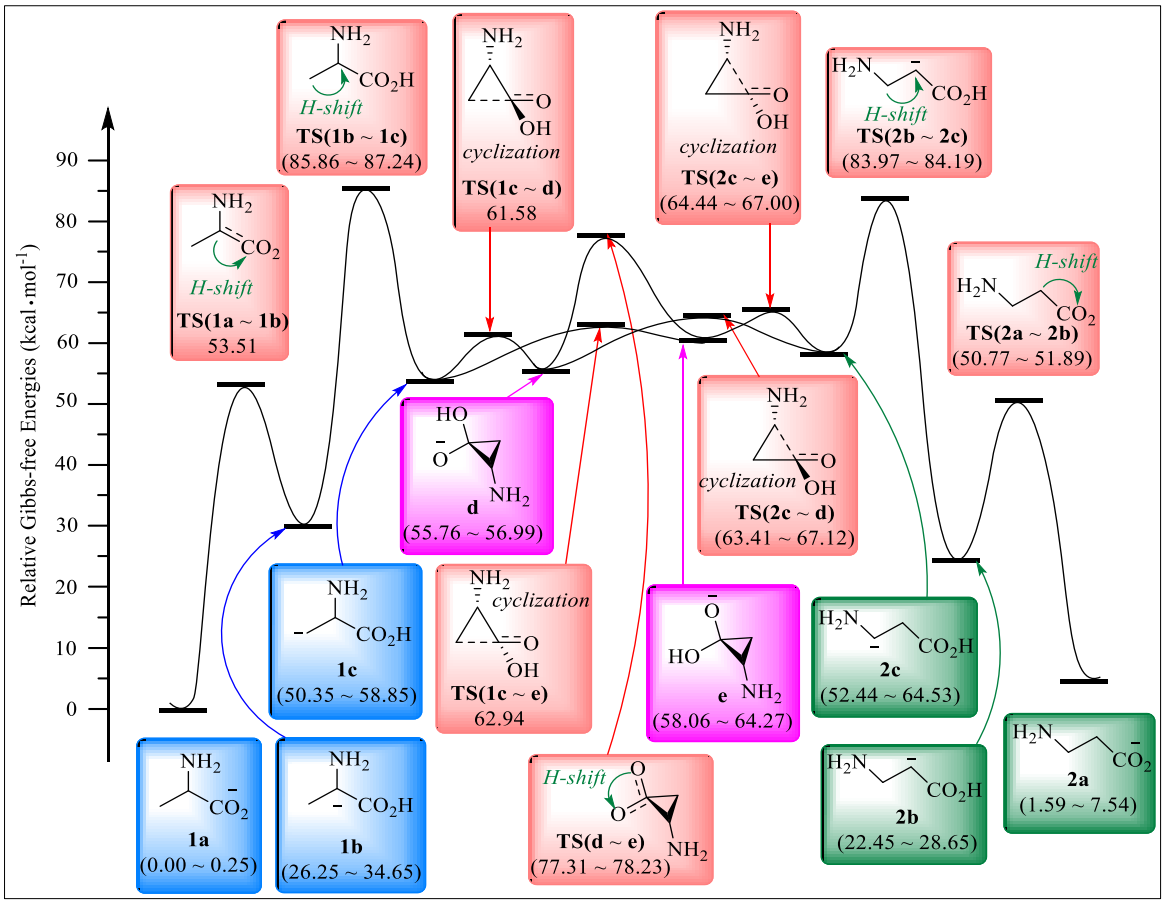

Figure 1: Ismerization potential energy profile of [Ala–H]⁻ computed at the B3LYP/6-311++G(2df,2pd) level of theory with the temperature of 473.15 K

As can be seen from this figure, in this six species isomers of [α-Ala–H]⁻ and [β-Ala–H]⁻, Gibbs free energies of **1a** and **1c** are less than **2a** and **2c**, which is consistent with the fact that α-alanine is more stable than β-alanine in neutral molecules [30]. The energy of **1b** is generally higher than that of **2b**. This is because when the negative charge is on α-C, **1b** ion exhibits $O\cdots C\cdots C_\alpha$ conjugation, while **2b** ion exhibits $O\cdots C\cdots C_\alpha\cdots C_\beta$ conjugation. The increase of the conjugate region of **2b** leads to lower energy and more stable structure. The energy of isomers from **1a (2a)** to

1b (2b) to **1c (2c)** increases in a step, indicating that the structure becomes more unstable as the negative charge migrates from the CO_2 region to α-C and then to β-C. When **1c (2c)** isomerize to **d** and **e**, while negative charge by β-C transfer back to the carboxyl, but species **1a (2a)** is CO_2^- form, negative charge free in between the two oxygen atoms, and with carboxyl carbon atoms form conjugate structure and **α-C**, and **d** and **e** negative charge is fixed on one atom of oxygen, which makes the **d** and **e** of the energy will not be reduced. The figure only shows the isomerization (hydrogen transfer and ion loop formation) between the categories. The reaction barrier ($\Delta G^{\neq}$) required for single rotation within the categories is generally not high, so it is not described here. From the hydrogen transfer process, it can be seen that the reaction barrier required for hydrogen transfer from **1b (2b)** to **1c (2c)** ($\Delta G^{\neq}$, 52.59 ~ 61.52 kcal·mol^{-1}) is higher than that from **1a (2a)** to **1b (2b)** ($\Delta G^{\neq}$, 50.77 ~ 53.51 kcal·mol^{-1}), which indicates that the energy required for hydrogen proton transfer from α-C to oxygen atom of carboxyl is higher than that from β-C to α-C. The energy required for hydrogen transfer between **d** and **e** is the lowest in the research system, which indicates that hydrogen protons on the carboxyl group are more active than hydrogen protons at other positions, which is also an important reason why CO_2^- is stable structure generated during amino acid hydrolysis or gas deprotonated dissociation. Isomerization from **1c(2c)** to **d** or **e** is an ion-forming process, and the reaction barrier required is lower than that for hydrogen proton transfer, which indicates that the energy required for electron transfer is lower than that for proton transfer. It can be seen clearly from the barriers of the proton transfer, the barriers of transition state ($\Delta G_{TS}^{\neq}$) of **1a** to **1b** is higher than **2a** to **2b**, the $\Delta G_{TS}^{\neq}$ of **1b** to **1c** is higher than **2b** to **2c**. This is due to the fact that the amino group is the electron donor group, and α-NH_2 is more efficient at providing electrons, which lowers the energy of the ionic system, making it more energy intensive for proton transfer. When the energy provided by the environment reaches 85.86 kca·mol^{-1}, the deprotonated α- and β-alanine ions can be converted to each other.

3.2 H_2O-loss Reaction of $[Ala–H]^-$

The potential energy profile of H_2O-loss pathways of $[Ala–H]^-$ were shown in Figure 2. All the energies given in the figure are relative Gibbs free energies (R.G., kcal·mol^{-1}) obtained with **1a2** as reference point.

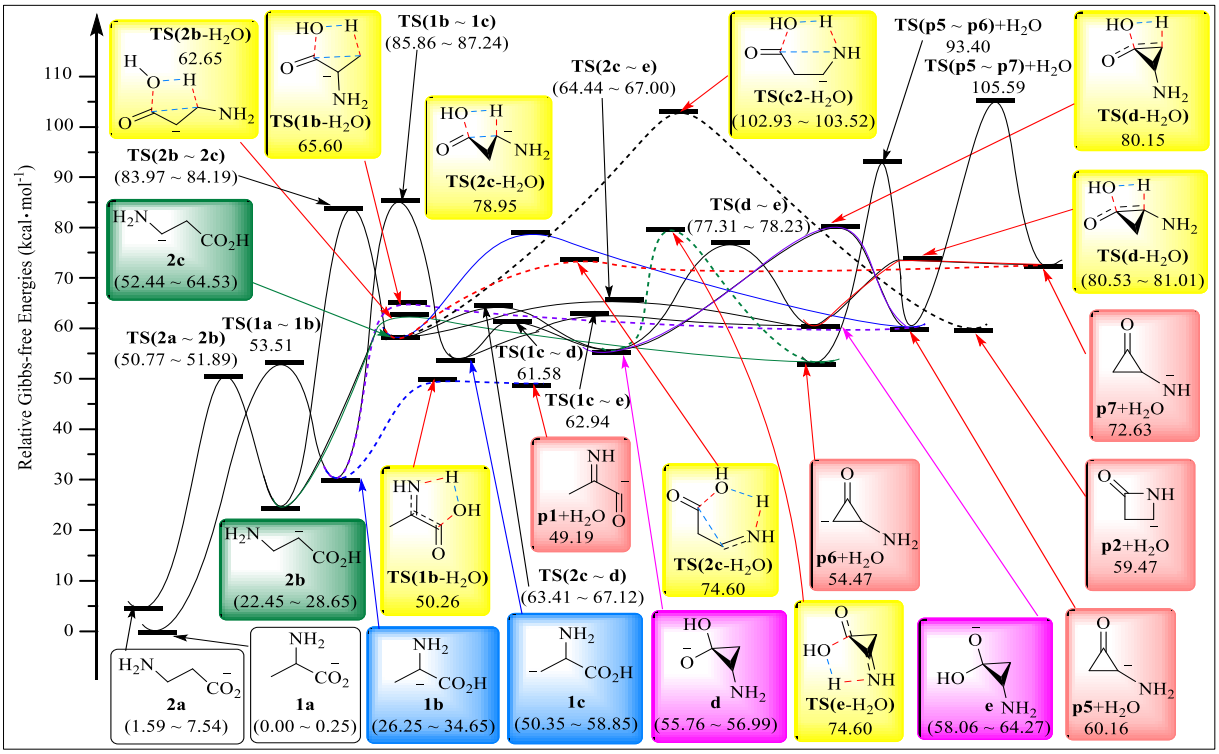

Figure 2: Potential energy profile of H_2O-loss fragmentation reaction computed at the B3LYP/6-311++G (2df,2pd) level of theory with the temperature of 473.15 K

As can be seen from Figure 2, the intermediate **1b** has two ways of H_2O-loss reaction. In the first case, the hydrogen on α-NH_2 and the hydroxyl group on the carboxyl group approach each other and dehydrate to form **p1**. In the second case, the β-C atom attacks the carboxyl carbon atom, causing the hydrogen atom to bond with the hydroxyl group and dehydrate to form **p5**. β- C of intermediate **2b** attacks carboxyl carbon, causing –OH group on carboxyl to combine with β-H and dehydrate, and then generate **p6** ion.

There are three dehydration modes of intermediate **2c**. The first mode is similar to the relative dehydration mode of **1b**, in which β-C atom attacks carboxyl carbon atom, causing hydrogen atom to bond with hydroxyl group, and dehydrates into cycle-formed **p5**. In the second way, β-C attacks the carboxyl carbon, causing the hydrogen of β-NH_2 to combine with the hydroxyl group in the carboxyl group and dehydrate to form **p7**. In the third case, the nitrogen from terminal group attacks the carbon atom from carboxyl group, causing the amino H atom to combine with the hydroxyl group on the carboxyl group and dehydrate to form the N-containing quaternary heterocyclic ion **p2**.

Intermediate **d** can be dehydrated in two ways. First, hydrogen on –NH_2 combines with –OH to dehydrate and produce **p6**. The second is that the hydrogen atoms on CH_2 combine with –OH and dehydrate to form **p5**. However, the intermediate **e** has only one way of H_2O-loss reaction, that is, hydrogen on CH_2 combines with –OH to dehydrate and produce **p7**.

In these paths, the ionic energy of all products is higher than that of the initial reactants, indicating that the H_2O-loss reaction is positive and non-spontaneous in thermodynamics. According to the dynamics, the path forming N-heterocyclic products has the highest energy (102.93 ~ 103.52 kcal·mol^{-1}) in the rate-determining step. The reaction path of product p1 formed from **1b** is the path of relative advantage in the H_2O-loss reaction of [α-Ala–H]$^-$, and the product obtained is also the most stable. The reaction path from **2b** to **p6** is the relative dominant path in the H_2O-loss reaction of [β-Ala–H]$^-$. The dominant H_2O-loss pathway of [α-Ala–H]$^-$ is lower than that of [β-Ala–H]$^-$, and its product ions are more stable than that of [β-Ala–H]$^-$. The product ions **p5**, **p6** and **p7** can be isomerized with each other by proton transfer, but the energy required for isomerization is above 93 kcal·mol^{-1}, which makes the isomerization process between the products difficult to realize.

3.3 NH_3-loss Reaction of [Ala–H]$^-$

The potential energy profile of NH_3-loss pathways of the deprotonated α- and β-alanine ions were shown in Figure 3. All the energies given in the figure are relative Gibbs free energies (R.G., kcal·mol^{-1}) obtained with **1a2** as reference point.

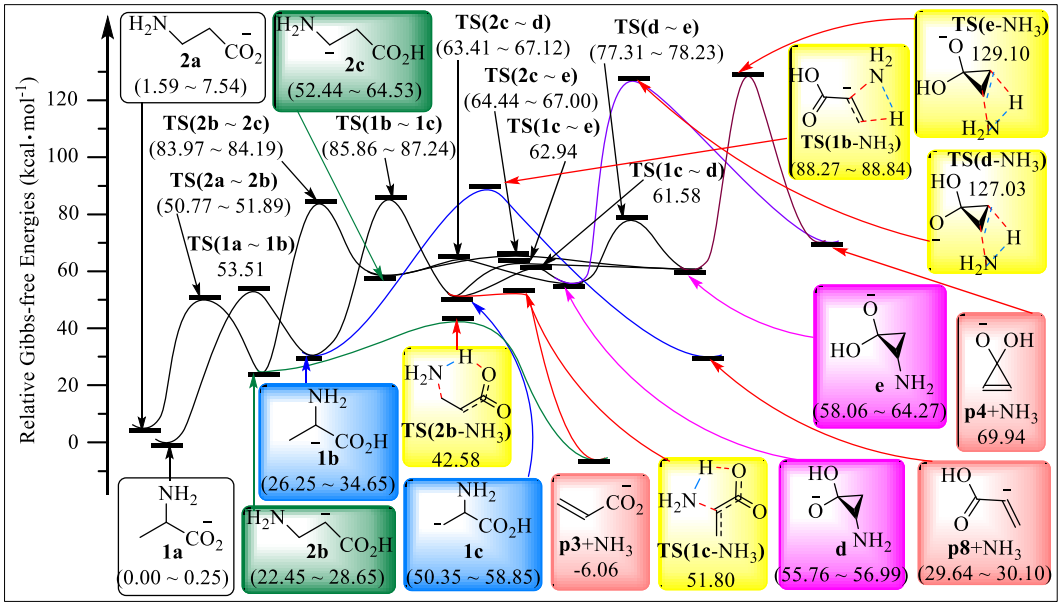

Figure 3: Potential energy profile of NH_3-loss fragmentation reaction computed at the B3LYP/6-311++G (2df,2pd) level of theory with the temperature of 473.15 K

It can be seen from Figure 3 that there are five modes of NH_3-loss reaction for [α-Ala–H]$^-$ and [β-Ala–H]$^-$. Product **p8** and NH_3 can be produced by α-NH_2 on intermediate **1b** with hydrogen on β-C. β-NH_2 on the intermediate **2b** can be delaminated with hydrogen on β-C to form **p3**, and α-NH_2 on **1c** can also be delaminated with hydrogen on carboxyl group to form the same product. **d** and **e** share a common NH_3-loss mode, that is, –NH_2 combines with hydrogen on –CH_2 to delaminate, and finally forms **p4**. According to reaction thermodynamics, the generated **p3** product is the only substance whose energy is lower than the initial reactant among all the deamination products. Therefore, only these two reaction paths are positive spontaneous processes, and the rest are positive non-spontaneous reactions. According to the reaction kinetics, the reaction path **1b (2b)** generates **p3** has a lower barrier than other NH_3-loss pathways, indicating that these two reaction paths are the most advantageous ones in NH_3-loss reaction of the deprotonated α- and β-alanine ions, respectively. When the energy provided by the system is higher than 85.86 kcal·mol^{-1}, the deprotonated α- and β-alanine ions can be isomerized with each other, and the reaction path from **2b** to **p3** is the most dominant path in the deamination reaction.

3.4 Temperature Dependence of the H_2O- and NH_3-Loss Reaction

In order to investigate the influence of temperature on the reaction pathways and products, the reference point **1a2**, the transition states of the rate-determining steps in the reaction pathways and transition states that are close to the energy of the rate-determining steps, the products after dehydration and deamination, and two neutral molecules, NH_3 and H_2O, were selected for frequency analysis and calculated the thermodynamic data. The selected temperature range is 273.15 ~ 853.15K, and the interval temperature is 20 K. The results are shown in Figure 4.

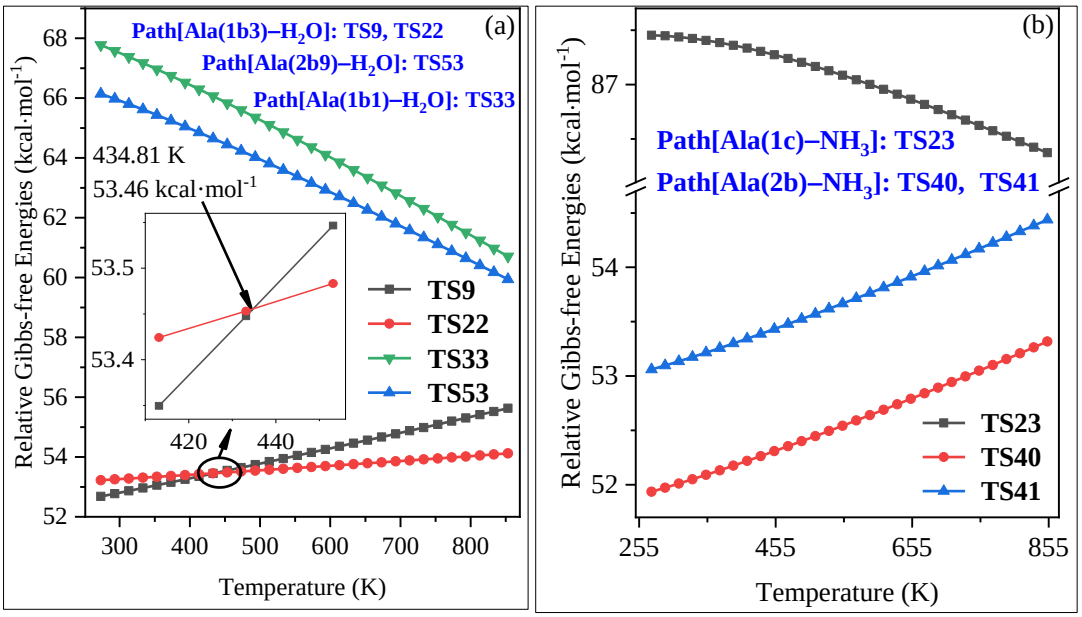

Figure 4: Temperature dependence of the rate-determining steps for the H_2O- (a) and NH_3-loss (b) reaction computed at the B3LYP/6-311++G (2df, 2pd) level of theory

It can be seen from Figure 4 that the influence of temperature on H_2O- (a) and NH_3-loss (b) reaction of $[Ala–H]^-$ over the dominant path is basically controlled within 10 kcal·mol^{-1}. Figure 4(a) shows the curve of the rate-determining steps of H_2O-loss reaction path changing with temperature, and Figure 4(b) shows the curve of the rate-determining steps of NH_3-loss reaction path changing with temperature.

As shown in Figure 4(a), the NH_3-loss reaction barrier of **2b9** and **1b1** decreases with the increase of temperature, while the barrier of **2b9** is always lower than that of **1b1**. According to kinetics, the NH_3-loss reaction of **2b9** is easier than that of **1b1**. However, the decisive step of H_2O-loss reaction of **1b3** is lower than that of **1b1** and **2b9**, indicating that H_2O-loss reaction of **1b3** is the best dehydration path in the whole kinetics. **TS9** and **TS22** are two possible rate-determination steps for **Path 2** because they have very similar energies. As can be seen from the figure, when the temperature is lower than 434.81 K, **TS22** is the rate-determining step of **Path 2**; when the temperature is higher than 434.81 K, **TS29** becomes the rate-determining step; and the reaction barrier ($\Delta G^{\neq}$) of H_2O-loss reaction is 53.46 kcal·mol^{-1} at 434.81 K.

As shown in Figure 4(b), **TS23** is the most advantageous path for the NH_3-loss reaction of $[\alpha$-Ala–$H]^-$, while **TS40** and **TS41** are the two possible decisive steps in the most advantageous path for the NH_3-loss reaction of $[\beta$-Ala–$H]^-$. Among the two NH_3-loss reaction pathways, **TS23** decreases with the increase of temperature, while the energy of **TS40** and **TS41** increases with the increase of temperature. **TS40** is always the rate-determine step in the most dominant path of NH_3-loss reaction of $[\beta$-Ala–$H]^-$, and the NH_3-loss reaction of $[\beta$-Ala–$H]^-$ is more advantageous than that of $[\alpha$-Ala–$H]^-$.

In conclusion, with the change of temperature, $[\alpha$-Ala–$H]^-$ has the most dominant chemical kinetic path in the H_2O-loss reaction of $[Ala–H]^-$. In the NH_3-loss reaction of $[Ala–H]^-$, $[\beta$-Ala–$H]^-$ has the most dominant pathway in chemical kinetics.

3.5 FPA of the Fragmentation Mechanism of $[Ala–H]^-$

Figure 5 shows the FPA of $[Ala–H]^-$ fragmentation mechanism at different calculation levels with 473.15K. This paper will use BH*and*HLYP [31], B97D [32], CBS-QB3 [33], G3MP2B3 [34], M062X [32] and MP2 [35] methods to compare with B3LYP calculation method. The methods CBS-QB3, G3MP2B3 and MP2 need to reduce the base set due to high memory consumption, and the calculation is completed under the base group of 6-311++G (d,p) [36], while the other four methods are completed under the base set of 6-311++G (2df,2pd).

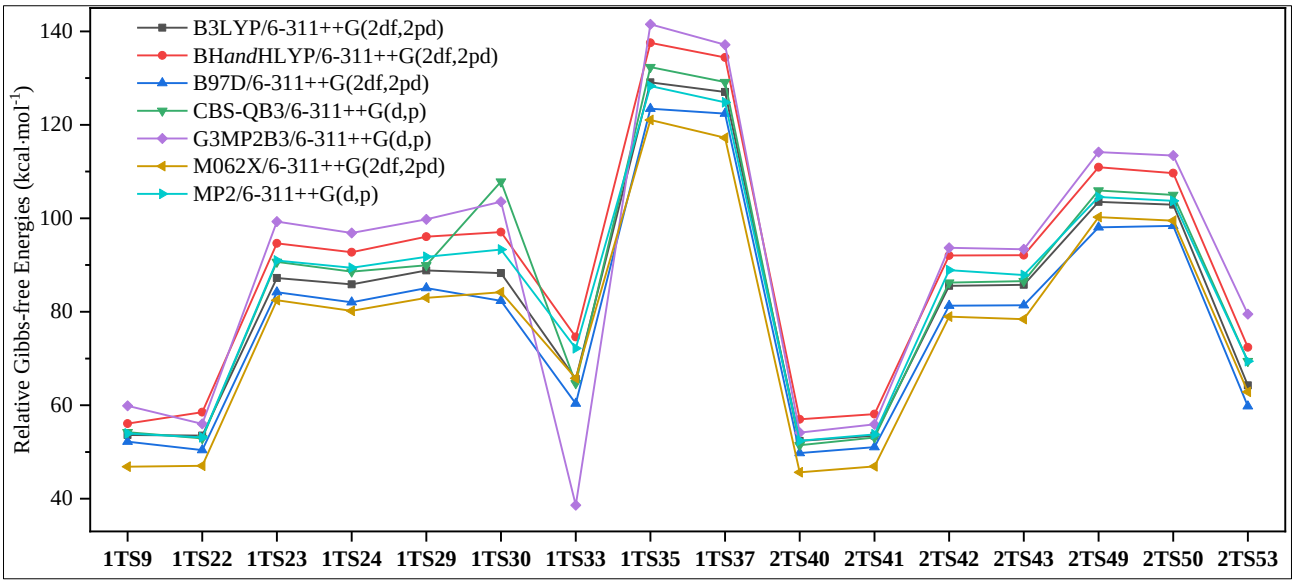

Figure 5: FPA of the fragmentation mechanism of [Ala–H]⁻

As can be seen from Figure 5, the hybrid algorithm G3MP2B3 has a large deviation in calculating the energy of **1TS22** and **1TS33**, while CBS-QB3 has a large deviation in calculating the energy of **1TS30**. According to the trend, the 7 calculation methods including B3LYP have basically the same trend. Only G3MP2B3 and B97D are different from other methods in the energy calculation of **1TS22** and **1TS30**, respectively. B3LYP also has a slight deviation in the calculation of **1TS30**, but the performance is not significant. This shows that the hybrid algorithm G3MP2B3 is not suitable for this system. Among the 7 methods, MP2 is more inclined to calculate the hydrogen bond, while M062X is more inclined to calculate the conjugation system of organic molecules. On the whole, B3LYP/6-311++G(2DF, 2Pd) level is more suitable for the calculation of the system.

4. CONCLUSION

The reaction mechanism of [Ala–H]⁻ at B3LYP/6-311++G(2df,2pd) level with the temperature of 473.15 K shows that H_2O- and NH_3-loss reaction could be realized when the energy provided by the environment was higher than 87.24 kcal·mol^{-1}. The details are listed below.

1. [α-Ala–H]⁻ is more stable than [β-Ala–H]⁻. During the isomerization of [Ala–H]⁻, the $\Delta G^{\neq}$ required for hydrogen transfer is higher. When the energy provided by the environment reached 85.86 kcal·mol^{-1}, the deprotonated α- and β-alanine ions could be converted to each other.
2. The dominant H_2O-loss pathway of [α-Ala–H]⁻ is from **1b**, and the corresponding product **p1** is also the most dominant product among all the dehydration products. The dominant H_2O-loss pathway of [β-Ala–H]⁻ is from **1b**. The dominant path of the NH_3-loss reaction of [α-Ala–H]⁻ is splitting NH_3 from **1b**, and that of [β-Ala–H]⁻ is splitting ammonia **2c**, and their corresponding products are the most dominant product **p3** in deamination products. According to chemical thermodynamics, the reaction path corresponding to deamination product **p3** is the unique reaction that can proceed spontaneously in the forward direction, and **p3** is also the most dominant product in both H_2O- and NH_3-loss reactions. However, according to the reaction kinetics, the NH_3-loss reaction path starting from **2c** has the lowest $\Delta G^{\neq}$ and is the most advantageous reaction path among all the reactions.
3. The dependence temperature in the range of 273.15 ~ 853.15 K only changed the rate-determining step of the optimal H_2O-loss path of [α-Ala–H]⁻.
4. FPA showed that B3LYP/6-311++G(2df, 2pd) level is suitable for the system

FUND PROJECT

"Three Longitudinal" Youth Innovative Talent Project of Heilongjiang Bayi Agricultural University (ZRCQC202010); Daqing City guiding science and technology project (zd-2021-88); Doctoral Research Foundation of Heilongjiang Bayi Agricultural University (XDB202112).

AUTHOR'S BRIEF INTRODUCTION

Quan Sun (1990-), man, Master's Degree, Assistant laboratory Technician, Corresponding author, mainly engaged in theoretical study on the reaction mechanism of substances.

REFERENCES

1. Rezaei, R., Wu, Z., Hou, Y., Bazer, F. W., & Wu, G. (2016). Amino acids and mammary gland development: nutritional implications for milk production and neonatal growth. *Journal of animal science and biotechnology*, *7*(1), 1-22.
2. Lu. J., Wang. G., & Wang, R. (2022). Progress in preparation of alanine [J/OL]. *Food and*

Fermentation Industries, 1-8.
3. Nelson, G., Chandrashekar, J., Hoon, M. A., Feng, L., Zhao, G., Ryba, N. J., & Zuker, C. S. (2002). An amino-acid taste receptor. *Nature*, *416*(6877), 199-202.
4. Kasschau, M. R., Skisak, C. M., Cook, J. P., & Mills, W. R. (1984). β-Alanine metabolism and high salinity stress in the sea anemone, Bunodosoma cavernata. *Journal of Comparative Physiology B*, *154*(2), 181-186.
5. Choquet, D., & Korn, H. (1988). Does β-alanine activate more than one chloride channel associated receptor?. *Neuroscience letters*, *84*(3), 329-334.
6. Sandberg, M., & Jacobson, I. (1981). β-Alanine, a possible neurotransmitter in the visual system?. *Journal of Neurochemistry*, *37*(5), 1353-1356.
7. Qiu, W., Soloshonok, V. A., Cai, C., Tang, X., & Hruby, V. J. (2000). Convenient, large-scale asymmetric synthesis of enantiomerically pure trans-cinnamylglycine and-α-alanine. *Tetrahedron*, *56*(17), 2577-2582.
8. Juaristi, E., & Soloshonok, V. (2005). Enantioselecti Ve Synthesis of -Amino Acids, *2nd ed, Wiley: New York.*
9. LIU, J., JIANG, C., LIU, F., GAO, F., ZHANG, X., LEI, Z., ... & WANG, Z. (2021). Theoretical study on the optical isomerization of α-alanine Mn (II) complex in water-liquid phase environment. *Journal of ZheJiang University (Science Edition)*, *48*(6), 700-710.
10. Meenukutty, M. S., Mohan, A. P., Vidya, V. G., & Kumar, V. V. (2022). Synthesis, characterization, DFT analysis and docking studies OFA novel schiff base using 5-bromo salicylaldehyde and β-alanine. *Heliyon*, e09600.
11. Delkov, D., Yoanidu, L., Tomov, D., Stoyanova, R., Dechev, I., & Uzunova, Y. (2022). Oncometabolites in urine-a new opportunity for detection and prognosis of the clinical progress of verified prostate cancer-a pilot study. *Turkish Journal of Medical Sciences*, *52*(3), 699-706.
12. Hong, J., Zhu, Z., Lu, H., & Qiu, Y. (2014). Synthesis and arsenic adsorption performances of ferric-based layered double hydroxide with α-alanine intercalation. *Chemical Engineering Journal*, *252*, 267-274.
13. Bellinger, P. M. (2014). β-Alanine supplementation for athletic performance: an update. *The Journal of Strength & Conditioning Research*, *28*(6), 1751-1770.
14. Moore, B., Toh, S. Y., Wong, Y. A., Bashiri, T., McKinnon, A., Wai, Y., ... & Momose, T. (2021). Hydrocarboxyl Radical as a Product of α-Alanine Ultraviolet Photolysis. *The Journal of Physical Chemistry Letters*, *12*(50), 11992-11997.
15. Blagojevic, V., Petrie, S., & Bohme, D. K. (2003). Gas-phase syntheses for interstellar carboxylic and amino acids. *Monthly Notices of the Royal Astronomical Society*, *339*(1), L7-L11.
16. Godfrey, P. D., Firth, S., Hatherley, L. D., Brown, R. D., & Pierlot, A. P. (1993). Millimeter-wave spectroscopy of biomolecules: alanine. *Journal of the American Chemical Society*, *115*(21), 9687-9691.
17. Attila, G. C. (1996). Conformers of Gaseous r-Alanine, *Journal of Physical Chemistry*, 100(9), 3541-3551.
18. McGlone, S. J., & Godfrey, P. D. (1995). Rotational Spectrum of a Neurohormone:. beta.-Alanine. *Journal of the American Chemical Society*, *117*(3), 1043-1048.
19. Zagórski, Z. P., & Sehested, K. (1998). Transients and stable radical from the deamination of α-alanine. *Journal of radioanalytical and nuclear chemistry*, *232*(1), 139-141.
20. Abraham, R. J., & Hudson, B. D. J. (1986). Rotational isomerism—XXI11 Pt XX, R. J. Abraham & P. Loftus, J. Chem. Soc. Perkin Trans. II, 1142 (1976). The conformation of 2-amino-3-fluoropropanoic acid (2-afp) and 2-fluoro-3-aminopropanoic acid (3-afp) as the zwitterion, cation and anion, an nmr a. *Journal of the Chemical Society*, Perkin Transactions. I1, 1635-1640.
21. Simpson, H. J., & Marsh, R. E. (1966). The crystal structure of L-alanine. *Acta Crystallographica*, *20*(4), 550-555.
22. Papavinasam, E., Natarajan, S., & Shivaprakash, N. C. (1986). Reinvestigation of the crystal structure of β-alanine. *International Journal of Peptide and Protein Research*, *28*(5), 525-528.
23. Eckersley, M., Bowie, J. H., & Hayes, R. N. (1989). Collision-induced dissociations of deprotonated α-amino acids. The occurrence of specific proton transfers preceding fragmentation. *International journal of mass spectrometry and ion processes*, *93*(2), 199-213.
24. Choi, S. S., & Kim, O. B. (2013). Fragmentation of deprotonated amino acids in atmospheric pressure chemical ionization. *International Journal of Mass Spectrometry*, *338*, 17-22.
25. Sun, Q., & Yu, H. T. (2018). A density functional theory investigation of the fragmentation mechanism of deprotonated asparagine. *Computational and Theoretical Chemistry*, *1141*, 45-52.
26. Allen, W. D., & Császár, A. G. (2010). The Composite Focal-Point Analysis (FPA) Approach. *Molecular Quantum Mechanics: From Methylene to DNA and Beyond*, 261-265.
27. Zhang, I. Y., Wu, J., & Xu, X. (2010). Extending the reliability and applicability of B3LYP. *Chemical Communications*, *46*(18), 3057-3070.
28. Miehlich, B., Savin, A., Stoll, H., & Preuss, H. (1989). Results obtained with the correlation energy density functionals of Becke and Lee, Yang and Parr. *Chemical Physics Letters*, *157*(3), 200-206.

29. Frisch, M. J., Trucks, G. W., Schlegel, H. B., Scuseria, G. E., Robb, M. A., Cheeseman, J. R., ... & Fox, D. J. (2009). Gaussian 09, Revision D. 01, Gaussian, Inc., Wallingford CT. *See also: URL: http://www. gaussian. com*.
30. Ribeiro da Silva, M. A., Ribeiro da Silva, M. D. D. M., Santos, A. F. L., Roux, M. V., Foces-Foces, C., Notario, R., ... & Juaristi, E. (2010). Experimental and computational thermochemical study of α-alanine (DL) and β-alanine. *The Journal of Physical Chemistry B*, *114*(49), 16471-16480.
31. Jursic, B. S. (1995). Theoretical investigation of cis-nitric oxide dimer with hybrid density functional theory methods. *Chemical physics letters*, *236*(3), 206-210.
32. Plumley, J. A., & Dannenberg, J. J. (2011). A comparison of the behavior of functional/basis set combinations for hydrogen-bonding in the water dimer with emphasis on basis set superposition error. *Journal of computational chemistry*, *32*(8), 1519-1527.
33. Pokon, E. K., Liptak, M. D., Feldgus, S., & Shields, G. C. (2001). Comparison of CBS-QB3, CBS-APNO, and G3 predictions of gas phase deprotonation data. *The Journal of Physical Chemistry A*, *105*(45), 10483-10487.
34. Anantharaman, B., & Melius, C. F. (2005). Bond additivity corrections for G3B3 and G3MP2B3 quantum chemistry methods. *The Journal of Physical Chemistry A*, *109*(8), 1734-1747.
35. Sharma, A., Verma, V. K., Singh, J. B., & Guin, M. Investigation of Intramolecular Hydrogen Bonding in Naphthoquinone Derivatives by Quantum Chemical Calculations. *Journal of Physical Organic Chemistry*, e4413.
36. Türker, L. (2022). Monomethoxy Isomers of Psoralen-DFT Treatment. *Earthline Journal of Chemical Sciences*, *8*(2), 175-192.